QUASI-STELLAR OBJECTS IN THE PARKES 2700 MHz SURVEY: THE SELECTED REGIONS AND THE ±4° DECLINATION ZONE

By J. G. Bolton* and J. V. Wall†

[*Manuscript received April* 9, 1970]

Abstract

One hundred and thirty-two quasi-stellar objects or possible quasi-stellar objects have been found in the first areas of the Parkes 2700 MHz survey. Identifications for 36 of these have already been published and 67 have been confirmed by spectroscopy or two-colour photography. Relationships between the various radio and optical parameters are briefly discussed.

I. Introduction

(*a*) *The* ±*4° Declination Zone*

In 1967 a new sky survey was begun with the 210 ft Parkes telescope and a sensitive 2700 MHz receiver. Some early results on source counts from the survey have been reported by Shimmins, Bolton, and Wall (1968). With an output time constant of 2 sec the receiver has peak-to-peak noise fluctuations of only 0·04 degK; this is equivalent to 0·07 f.u.‡ on the 210 ft telescope. A survey of the zone between declinations +4° and −4° (excluding two areas near the galactic plane) was made by scanning the telescope in right ascension at intervals of 6′ arc in declination. The scan rate was 2° per min with a receiver output time constant of 1 sec. A dual feed system was used which produced an on-axis beam, 7′·9 arc between half-power points, and another of similar width displaced in declination by 18′ arc. The difference in signal between the two feeds was recorded. All sources estimated to have flux densities $\geqslant 0\cdot 3$ f.u. from the survey records were selected for further measurements, which included accurate positioning and spectral observations. For the latter, flux densities were measured at some or all of the following frequencies: 467, 635, 1410, and 5000 MHz. The observations at 635 and 5000 MHz were made with the 210 ft telescope. The observations at 467 and 1410 MHz were made with the Parkes interferometer using the 60 ft telescope in conjunction with the 210 ft telescope. Accurate positions were measured at 2700 MHz with the 210 ft telescope and known quasi-stellar objects (QSOs) with accurate optical positions in the ±4° zone were used as calibration sources. The positions have an estimated r.m.s. accuracy of 10″ arc. Full details of the observations and the resulting catalogue are to be published by Wall, Shimmins, and Jeannette K. Merkelijn.

* Division of Radiophysics, CSIRO, P.O. Box 76, Epping, N.S.W. 2121.

† Mount Stromlo and Siding Spring Observatories, Research School of Physical Sciences, Australian National University, Canberra, A.C.T. 2600.

‡ 1 flux unit (f.u.) = 10^{-26} W m^{-2} Hz^{-1}.

In order to secure positive identification of QSOs in the survey zone a series of two-colour plates was taken with the 48 in. Schmidt telescope at Palomar Observatory in 1966 and 1968 by J.G.B. Kodak 103a-0 plates were used and an exposure of 8 min was made behind a GG-13 (minus u.v.) filter followed by an exposure of 60 min behind a UG-1 (u.v.) filter. The telescope was displaced by 12″ arc in right ascension between the two exposures. On most of these plates a stellar object with an ultraviolet excess greater than U−B = −0·4 has an ultraviolet image brighter than the blue image. Plates which were taken under conditions of good seeing have a limit in the blue which is about half a magnitude brighter than the standard blue Sky Survey plates. Unfortunately it was not possible to secure plates to cover the entire area of the radio survey. No plates were obtained between right ascensions 14^h and 17^h, and the plates cover 6°40′ in declination compared with the 8° in declination of the radio survey. The areas covered by the photographic and radio surveys are shown in Figure 1.

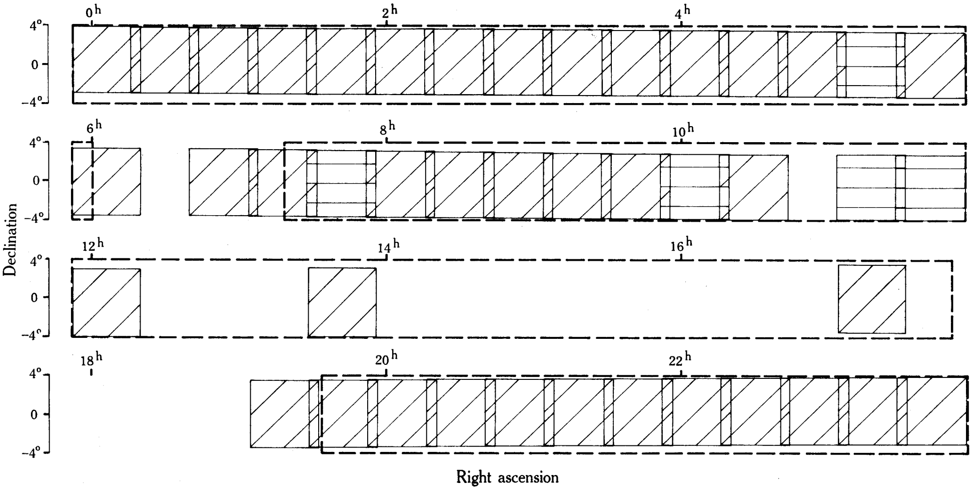

Fig. 1.—Areas in the ±4° declination zone covered by the radio survey (enclosed by heavy dashed lines) and the two-colour plates. Plate areas shown diagonally hatched were taken under conditions of good seeing and those horizontally hatched under conditions of poor seeing.

(b) *Selected Areas*

The survey of the ±4° zone is thought to be complete to a flux density of 0·35 f.u. at 2700 MHz, although many sources ⩾0·25 f.u. are included in the catalogue. In addition to the ±4° survey, deeper surveys with a nominal lower limit of 0·08 f.u. were made of six selected areas centred on 48 in. Sky Survey centres. The plates for these areas were amongst a number which were taken in 1966 under conditions of good seeing in regions free from galactic obscuration. Five of these are in the survey zone described previously and one is at declination −18°. The plate centres are listed in Table 1. The selected areas were surveyed by making scans at 1° per min in both right ascension and declination with a scan spacing of 4′ arc. Position measurements were subsequently made of all sources whose flux densities were estimated to be greater than 0·06 f.u. from the survey records. At the nominal lower limit of 0·08 f.u. the source density is about one source per square degree and confusion affects the accuracy of the position measurements. The combined effects of confusion and the low signal-to-noise ratio increase the estimated r.m.s. errors in position from about 10″ arc at 0·3 f.u. to about 30″ at 0·08 f.u.

TABLE 1

CENTRES OF SELECTED REGIONS

Plate Number	Position (1950·0) R.A. h m s	Dec. ° ′	Plate Number	Position (1950·0) R.A. h m s	Dec. ° ′
PS 1112	00 04 51	+00 32	PS 1777	12 04 50	−00 31
PS 891	00 52 55	+00 31	PS 1778	13 40 48	−00 29
PS 1114	02 32 31	+00 25	PS 896	22 03 26	−18 50

II. Identification of QSOs

The Palomar Sky Survey prints and the two-colour plates, where available, were examined in the positions of the 500 sources in the ±4° zone catalogue and the 300 sources in the selected-area catalogue. The examination was made with the aid of computer-drawn transparent overlays containing the positions of the radio source and 10 reference stars from the Smithsonian catalogue. Radio galaxies found in this examination have been published by Merkelijn and Wall (1970).

In most cases where two-colour plates were available a positive identification of a radio source as a QSO could be made from the close positional agreement between the source and a stellar object with obvious ultraviolet excess. In the identification tables such objects are denoted by "u.v.x." in the remarks column. Identifications for which the ultraviolet excess is less certain are indicated by "u.v.x.?". In some cases these are objects which are noticeably brighter on the blue Sky Survey print than on the red but which have almost equal images on the two-colour plate. These may be QSOs having u.v. excess close to the known lower limit of $\sim -0\cdot4$, due perhaps to a strong emission line in the blue region of the spectrum. In other cases where the plate was taken under conditions of poor seeing, the ultraviolet images are degraded and the colour balance of the plate upset; however, u.v. excess is suggested from a comparison of the relative image intensities of the object in question and other objects of the same blue intensity within a radius of 20′ arc.

In the region not covered by two-colour plates identifications are suggested on the basis of coincidence in position between the source and an object which is relatively brighter on the blue than on the red Sky Survey print. On the basis of such coincidences in the region where two-colour plates taken later subsequently rejected or confirmed the identification, it is probable that two-thirds of the suggested identifications are correct.

One hundred and three of the sources in the ±4° zone were found to be QSOs or possible QSOs. Identifications for 36 of these have already been published, 11 of which resulted from the present program; another 36 are confirmed from the two-colour plates and redshifts for 6 of these have been obtained; a further 31 identifications are suggested but not confirmed. In the selected areas an additional 29 QSOs were found, all confirmed by their ultraviolet excess.

TABLE 2

QUASI-STELLAR OBJECT IDENTIFICATIONS IN SELECTED REGIONS, 2700 MHz SURVEY

(1) PKS Source Number	(2) Optical Position (1950·0) R.A. h m s	(3) Dec. ° ′ ″	(4) Optical—Radio Coordinate Differences R.A. s	(5) Dec. ′	(6) m_v	(7) S_{2700} (f.u.)	(8) Spectral Index	(9) References*	(10) Other Catalogue Number	(11) Galactic Coordinates l^{II} °	(12) b^{II} °	(13) Remarks*
PS 1112												
0003−00	00 03 48·70	−00 21 06·6			19·5	2·41	0·80	25	3C 2	99	−61	z = 1·037 (20), optical variable (25)
0006+014	00 06 19·0	+01 25 20	2·0 p	0·6 n	18·5	0·09				101	−59	u.v.x.
PS 891												
0041+001	00 41 00·0	+00 08 30	1·9 p	0·6 s	19	0·08				118	−62	u.v.x.
0045−000	00 45 46·0	−00 01 06	1·3 p	0·2 n	19	0·11				121	−63	u.v.x.?
0056−00	00 56 31·70	−00 09 16			17·3	(1·80)	0·45	5, 10	4C−00·6	127	−63	z = 0·717 (21)
0057+028	00 57 34·5	+02 49 00	0·1 p	0·6 s	19·5	0·06				127	−60	u.v.x., optical variable
0103−021	01 03 48·6	−02 11 48	—	—	19	0·42	0·50			131	−64	u.v.x.
PS 1114												
0222+000	02 22 34·3	+00 03 24	0·5 f	0·1 n	19	0·14				166	−55	u.v.x.
0223+012	02 23 34·0	+01 16 06	0·5 f	—	19	0·24				165	−53	u.v.x.
0225−014	02 25 35·0	−01 29 06	0·5 p	—	18	0·30	0·8		4C−01·11	168	−55	z = 0·685 (9)
0231+022	02 31 14·6	+02 16 18	1·3 p	0·5 s	17·5	0·07				171	−54	u.v.x.
0232−02	02 32 59·9	−02 32 24	—	—	18	0·58	0·85		4C−02·12	172	−55	u.v.x.
0237−027	02 37 14·2	−02 47 12	1·0 f	—	18·5	0·41	−0·70			174	−54	u.v.x., inverted spectrum, optical variable?
0240−021	02 40 15·0	−02 10 24	—	0·2 n	19·5	0·12				174	−53	u.v.x.?, object 4^s f has u.v.x.
PS 1777												
1158+007	11 58 49·7	+00 45 10	0·4 f	0·3 s	18·5	0·26				276	61	u.v.x.
1159−036	11 59 38·4	−03 37 50	1·1 p	0·3 n	19·5	0·12				280	57	u.v.x.
1201−026	12 01 08·6	−02 37 55	0·9 f	0·3 s	19	0·15			4C−02·51	280	58	Optical variable
1203+011	12 03 15·3	+01 10 27	0·9 p	0·4 n	18	0·13				278	61	u.v.x.
1211+003	12 11 22·9	+00 22 29	1·2 p	0·5 s	20	0·10				283	61	u.v.x.
1216−010	12 16 01·0	−01 03 28	1·3 f	0·3 n	19·5	0·21				286	60	u.v.x.?
1217+02	12 17 38·35	+02 20 20·9	1·3 f	—	16·5	0·47	−0·05	3		284	65	z = 0·240 (22), h.f. enhancement

PS 1778												
1328−034	13 28 54·0	−03 25 54	2·5 p	0·2 n	19	0·26				321	58	u.v.x.
1331+004	13 31 07·7	+00 25 42	0·9 f	—	20	0·14				325	60	u.v.x.
1331+025	13 31 17·3	+02 34 06	0·9 p	0·2 n	18·5	0·14				326	63	u.v.x.
1335+023	13 35 06·9	+02 22 17	0·4 f	0·2 s	17·5	0·10				329	63	$z = 0·61$ (9)
1336−000	13 37 00·3	−00 00 54	0·5 p	0·3 s	19	0·11				328	60	u.v.x.
1337−013	13 37 30·4	−01 22 36	0·3 p	0·3 n	18·5	0·19				327	59	$z = 1·607$ (23)
1343+011	13 43 48·0	+01 09 13	0·2 p	1·0 n	20	0·10				332	61	Below limit of 2-colour plate
1352+00	13 52 34·7	+00 55 13	0·6 f	0·3 n	19	0·35	1·15	23		336	60	u.v.x.?, inverted spectrum
PS 896												
2153−204	21 53 47·1	−20 26 50	1·5 f	0·2 n	17	0·22		27		33	−50	$z = 1·31$ (27)
2156−183	21 56 31·6	−18 21 53	3·0 f	0·3 s	19·5	0·09				36	−49	u.v.x.
2157−200	21 57 21·7	−20 00 15	0·1 f	0·1 s	19·5	0·13				32	−50	u.v.x., optical variable
2159−215	21 59 05·7	−21 32 41	2·0 p	0·4 n	19	0·13				32	−51	u.v.x., finding chart from red print
2203−18	22 03 25·8	−18 50 16			19·5	5·20	0·40	5, 19	MSH 22−1*1*	36	−51	u.v.x.?

* References are: 1, present paper; 2, Bolton (1968); 3, Bolton *et al.* (1965); 4, Bolton and Ekers (1966*a*); 5, Bolton and Ekers (1966*b*); 6, Bolton and Ekers (1966*c*); 7, Bolton and Ekers (1967); 8, Bolton and Kinman (1966); 9, Bolton, Kinman, and Wall (1968); 10, Bolton *et al.* (1966); 11, Bolton, Shimmins, and Merkelijn (1968); 12, Bolton and Wall (1969); 13, Burbidge (1966); 14, Burbidge and Kinman (1966); 15, Clarke, Bolton, and Shimmins (1966); 16, Hazard, Mackey, and Shimmins (1963); 17, Jefferys (1964); 18, Kinman (personal communication); 19, Kinman *et al.* (1967); 20, Kinman and Burbidge (1967); 21, Lynds (1967); 22, Lynds *et al.* (1966); 23, Lynds (personal communication); 24, Merkelijn (1969); 25, Sandage, Véron, and Wyndham (1965); 26, Schmidt (1963); 27, Searle and Bolton (1968); 28, Shimmins *et al.* (1968); 29, Smith and Hoffleit (1963).

TABLE 3

QUASI-STELLAR OBJECT IDENTIFICATIONS IN DECLINATION ZONE +4° TO −4°, 2700 MHz SURVEY

(1) PKS Source Number	(2) Optical Position (1950·0) R.A. h m s	(3) Dec. ° ′ ″	(4) Optical—Radio Coordinate Differences R.A. s	(5) Dec. ′	(6) m_V	(7) S_{2700} (f.u.)	(8) Spectral Index	(9) References*	(10) Other Catalogue Number	(11) Galactic Coordinates l^{II} °	(12) b^{II} °	(13) Remarks*
0003−00	00 03 48·70	−00 21 06·6			19·5	2·41	0·80	25	3C 2	99	−61	z = 1·037 (20), optical variable (25)
0038−020	00 38 23·8	−02 02 54	—	0·2 n	18	0·61	−0·40			117	−64	z = 1·176 (1), inverted spectrum
0056−00	00 56 31·70	−00 09 16			17·3	(1·80)	0·45	5, 10	4C−00·6	127	−63	z = 0·717 (21)
0103−021	01 03 48·6	−02 11 48	—	—	19	0·42	0·50			131	−64	u.v.x.
0106+01	01 06 04·39	+01 19 01·9			18·4	(1·88)	−0·65	3, 2	4C+01·2	132	−61	z = 2·107 (13), h.f. enhancement
0112−017	01 12 43·5	−01 43 01	0·9 f	0·1 n	18	1·38	−0·25			136	−64	u.v.x., h.f. enhancement
0115+02	01 15 42·8	+02 42 35	0·2 f	0·5 s	17·5	0·88	0·85	11	4C+02·4	136	−59	z = 0·673 (27)
0118+03	01 18 26·15	+03 28 29·3			18	0·51	1·20	15, 2	4C+03·2	137	−58	z = 0·765 (1)
0122−00	01 22 55·5	−00 21 34			17	1·43	0·25	5, 10		140	−62	z = 1·070 (21), h.f. enhancement, l.f. cutoff
0137+012	01 37 22·8	+01 16 29	0·2 f	0·1 n	17·5	1·07	0·50		4C+01·4	147	−59	u.v.x.
0158+031	01 58 05·0	+03 08 14	—	—	19	0·28				154	−55	u.v.x.
0215+015	02 15 13·4	+01 30 56	0·6 f	—	18·5	0·36	0·23	12	OD 026	162	−54	Optical variable (12), l.f. cutoff
0225−014	02 25 35·0	−01 29 07	0·5 p	—	18	0·30	0·8	9	4C−01·11	168	−55	z = 0·685 (9)
0226−038	02 26 22·5	−03 50 58	0·7 f	0·1 s	17·5	0·66	0·30		4C−03·7	172	−57	z = 0·695 (1), h.f. enhancement
0232−02	02 32 59·9	−02 32 23	—	—	19	0·58	0·85	23	4C−02·12	172	−55	u.v.x.
0237−027	02 37 14·2	−02 47 34	0·3 f	0·4 n	19·5	0·41	−0·70			174	−54	u.v.x., inverted spectrum
0253−031	02 53 20·0	−03 11 37	0·2 f	—	19	0·29	1·15		4C−03·10	179	−52	
0256−005	02 56 54·8	−00 31 52	0·4 p	—	17·5	0·31	0·55			177	−49	u.v.x.
0300−00	03 00 39·5	−00 26 38	1·3 p	—	18·5	0·67	0·95		4C−00·14	178	−48	u.v.x.?, galaxy previously suggested (7)
0312−03	03 12 51·9	−03 27 51	0·2 f	0·1 n	18·5	0·68	1·10		4C−03·11	184	−48	u.v.x.
0317−02	03 17 56·5	−02 19 24	0·6 f	0·3 n	19·5	0·36	0·45		4C−02·15	184	−46	u.v.x., h.f. enhancement
0336−01	03 36 59·2	−01 56 19			18·4	(2·23)	−0·10	5, 19	CTA 26	188	−42	z = 0·852 (1), optical variable (19), l.f. cutoff
0351−032	03 51 43·3	−03 16 43	0·4 f	0·1 s	19·5	0·46	1·15		4C−03·14	192	−40	
0420+022	04 20 16·8	+02 12 24	0·2 p	0·1 n	19·5	0·34	−0·40			191	−31	u.v.x., inverted spectrum
0420−01	04 20 43·1	−01 27 29			18	(1·92)	−0·10	6, 18		195	−33	z = 0·915 (1) h.f. enhancement
0421+019	04 21 33·0	+01 57 33	1·0 f	0·1 n	17·5	0·76	0·20		OF 036	192	−31	z = 0·689 (1), l.f. cutoff
0440−00	04 40 05·4	−00 23 22			19·2	(3·53)	0·10	6, 18	NRAO 190	197	−29	u.v.x., inverted spectrum
0442−00	04 43 01·4	−00 24 53	0·2 p	0·3 n	20	0·27	0·4		DA 146	198	−28	u.v.x.
0445−019	04 45 11·2	−01 58 02	0·2 f	—	19	0·20				200	−28	u.v.x.
0447−010	04 47 10·1	−01 02 32	—	0·1 n	19·5	0·29	0·50			199	−27	u.v.x.

0454+039	04 54 08·8	+03 56 13	1·6 f	0·2 n	16·5	0·40	0·15		OF 092	195	−23	
0457+024	04 57 16·5	+02 25 02	0·9 p	—	19	1·63	0·20		OF 097	197	−23	u.v.x.?, inverted spectrum
0505+03	05 04 59·1	+03 04 00	0·6 f	0·1 s	19	0·74	0·50	23	4C+03·10	198	−21	u.v.x.?, galaxy previously suggested (15)
0736−01	07 36 02·6	−01 57 30	0·9 p	0·2 n	18	0·64	0·8		4C−01·18	219	10	u.v.x.
0736+01	07 36 42·4	+01 43 57			18	(2·42)	0·10	4, 8	OI 061	217	11	z = 0·191 (21), l.f. cutoff
0743−006	07 43 21·0	−00 36 57	0·2 p	0·1 s	18	1·40	−0·40		4C−00·28?	220	12	u.v.x.?, inverted spectrum
0808+019	08 08 51·1	+01 55 47	0·1 p	—	18	(0·71)	−0·40		OJ 014	221	19	u.v.x.?, inverted spectrum
0812+02	08 12 47·20	+02 04 11			18·5	1·18	0·70	15, 10	4C+02·23	222	19	z = 0·406 (20)
0828−03	08 28 15·2	−03 30 40	1·1 p	0·1 n	18·5	0·53	0·85		4C−03·32	228	20	u.v.x.
0837+035	08 37 12·6	+03 30 31	0·2 f	0·2 s	20	0·69	0·25		OJ 063	223	25	l.f. cutoff
0837+012	08 37 14·3	+01 15 08	0·1 p	0·3 n	19	0·25	−0·05		OJ 062	225	24	u.v.x.
0853+03	08 53 01·3	+03 23 52	0·6 p	0·1 s	17·5	0·35	1·00	23		225	29	l.f. cutoff
0906+01	09 06 35·3	+01 33 40	0·7 f	0·1 n	17·5	1·20	0·25	11	4C+01·24	229	31	u.v.x.
0907−023	09 07 13·6	−02 19 10	0·2 f	0·4 s	18	0·57	0·50			233	29	u.v.x.
0912+029	09 12 01·4	+02 58 37	0·4 f	0·1 n	18·5	0·54	0·25		OK 020	228	33	l.f. cutoff
0913−025	09 13 48·5	−02 32 02	—	0·4 n	18·5	0·28	0·9		4C−02·38	234	30	u.v.x.
0922+005	09 22 34·1	+00 32 09	0·3 f	0·1 s	18	0·74	0·05	9	OK 037	232	34	z = 1·72 (9), inverted spectrum
0932+02	09 32 42·9	+02 17 35	0·8 p	0·3 s	17·4	0·53	0·85	9	4C+02·27	232	37	z = 0·659 (9)
0950+00	09 50 12·0	+00 14 30	1·3 f	—	20	0·43	1·50	12		238	39	u.v.x., optical variable (12)
0957+00	09 57 43·84	+00 19 50·0			17·6	0·51	0·75	3	4C+00·34	239	41	z = 0·907 (22)
1004−018	10 04 31·6	−01 52 37	0·7 f	0·1 s	19	0·56	−0·10			243	41	u.v.x., l.f. cutoff
1008+013	10 08 41·5	+01 21 35	0·2 f	0·1 n	19	0·24	0·70		OL 014	240	44	u.v.x.
1012+022	10 12 41·6	+02 13 50	0·7 p	0·2 n	18	0·40	0·40		4C+02·30	240	45	u.v.x.
1021+028	10 21 18·0	+02 48 18	0·7 f	0·1 n	19	0·22				242	47	l.f. cutoff
1021−00	10 21 57·0	−00 37 36	1·2 p	—	18·5	0·95	0·30	7		245	45	u.v.x.?, inverted spectrum
1052−004	10 52 23·3	−00 29 54	0·4 p	0·2 n	18	0·34	0·95		4C−00·41	253	50	
1055+01	10 55 55·5	+01 50 03			18·3	(3·02)	0·00	15, 10	4C+01·28	251	53	u.v.x., h.f. enhancement
1103−006	11 03 58·0	−00 36 40	0·7 f	0·1 n	16·5	0·68	0·70		4C−00·43	257	52	u.v.x.
1105−028	11 05 03·9	−02 51 55	0·4 f	—	19·5	0·36	1·05		4C−02·45	259	51	
1106−003	11 06 18·3	−00 22 23	0·9 p	0·1 s	19·5	0·26	0·8			257	53	
1111−037	11 11 58·0	−03 44 47	0·5 f	0·2 n	18·5	0·35	0·7		4C−03·41	262	51	18m galaxy also near position
1130+009	11 30 46·6	+00 57 25	0·7 f	—	19	0·32	0·50			264	57	l.f. cutoff
1146−037	11 46 22·5	−03 47 29	1·4 f	—	17	0·40	0·35			274	55	
1148−00	11 48 10·23	−00 07 13·1			17·6	2·56	0·40	6, 2	4C−00·47	272	59	z = 1·982 (14), inverted spectrum
1217+02	12 17 38·35	+02 20 20·9	1·3 f	—	16·5	0·47	−0·05	3		284	65	z = 0·240 (22), h.f. enhancement
1218−02	12 18 51·0	−02 25 12	0·5 f	0·4 s	20	0·54	0·20	12	4C−02·53	288	59	u.v.x., optical variable (12), h.f. enhancement
1222+037	12 22 19·0	+03 47 24	0·2 f	0·1 n	19	0·81	−0·10		4C+03·23	287	65	h.f. enhancement
1225−02	12 25 22·7	−02 20 30	1·8 f	0·2 n	19·5	0·40	0·80		4C−02·54	291	59	u.v.x.
1226+02	12 26 33·3	+02 19 44			12·8	(43·4)	0·05	16, 17	3C 273	289	65	z = 0·158 (26), optical variable (29)
1229−02	12 29 25·9	−02 07 31			16·8	1·33	0·45	6, 8	4C−02·55	293	60	z = 0·388 (20), h.f. enhancement
1302−035	13 02 08·9	−03 29 56	—	0·2 s	19·5	0·53	0·60			309	59	

* For references see footnote at end of Table 2.

TABLE 3 (*Continued*)

(1) PKS Source Number	(2) Optical Position (1950·0) R.A. h m s	(3) Dec. ° ′ ″	(4) Optical–Radio Coordinate Differences R.A. s	(5) Dec. ′	(6) m_V	(7) S_{2700} (f.u.)	(8) Spectral Index	(9) References*	(10) Other Catalogue Number	(11) Galactic Coordinates l^{II} °	(12) b^{II} °	(13) Remarks*
1317−00	13 17 04·5	−00 34 18	0·4 p	0·1 n	17·3	0·97	0·55	9	4C−00·50	318	61	$z = 0·89$ (9)
1352+00	13 52 34·7	+00 55 13	0·6 f	0·3 n	19	0·35	1·15	23		336	60	u.v.x.?, inverted spectrum
1356+022	13 56 55·1	+02 14 17	—	0·2 s	18·5	0·66	0·45			339	60	Inverted spectrum
1359+039	13 59 54·2	+03 57 13	1·3 p	0·2 s	19	0·33	0·3			341	60	
1402−012	14 02 11·5	−01 16 13	0·2 f	0·1 n	18·5	0·71	−0·25			338	57	Inverted spectrum
1407+022	14 07 32·5	+02 17 16	0·1 f	—	19	0·49	0·10			343	59	
1424+03	14 25 02·1	+03 29 27	0·8 f	0·3 s	19	0·33	0·9		4C+03·29	351	57	
1449−012	14 49 12·1	−01 15 15	0·4 f	0·1 s	18	0·35	0·30			354	50	
1454−034	14 54 32·8	−03 27 48	1·1 p	—	19	0·29	0·9		4C−03·53	352	47	Brighter object with jet 0′·5 n.f. is within error of radio position
1502+036	15 02 35·9	+03 38 04	0·1 p	0·3 n	19	0·48	−0·40			2	50	Inverted spectrum
1514+00	15 14 06·0	+00 25 51	1·6 f	0·2 s	18·8	(1·83)	0·50	8, 11	4C+00·56	2	46	Part of flux due to nearby galaxy
1543+005	15 43 38·1	+00 35 37	0·9 p	0·1 s	19	1·30	0·55		DW1543+00	8	40	l.f. cutoff
1546+027	15 46 58·4	+02 46 07	1·2 p	0·2 s	18	(1·27)	−0·35			11	41	Inverted spectrum
1602−00·2	16 02 22·0	−00 11 02	2·0 f	0·5 s	18	(0·53)	0·40	23	DA 397	10	36	h.f. enhancement
1611−007	16 11 53·5	−00 47 58	0·4 p	0·1 n	18·5	0·27	0·9		4C−00·64	11	34	
1615+029	16 15 18·8	+02 53 58	0·4 p	0·1 n	18	0·74	0·15			16	35	
1618+007	16 18 15·3	+00 43 55	0·4 f	—	18·5	0·21				14	33	
1729+010	17 29 48·8	+01 01 45	0·4 p	0·3 n	19	0·20	1·0		4C+01·52	24	18	
1942+038	19 42 06·0	+03 49 30	1·2 f	0·1 n	17·5	0·50	0·80		4C+03·46	43	−10	
1952+007	19 52 49·8	+00 42 04	0·4 f	0·1 n	18·5	0·34	0·80		4C+00·74	41	−14	u.v.x.?
1953+035	19 53 03·7	+03 36 04	4·4 f	0·3 s	18	0·29	1·15		4C+03·47	43	−12	
2059+034	20 59 08·8	+03 29 49	—	—	18	0·59	−0·35			53	−27	u.v.x., inverted spectrum
2110−017	21 10 12·2	−01 46 28	0·9 f	0·1 n	19·5	0·31	0·8		4C−01·55	49	−32	u.v.x.
2131−021	21 31 35·3	−02 06 36	1·8 p	—	19	1·91	−0·10		4C−02·81	52	−36	u.v.x., h.f. enhancement
2134+004	21 34 05·3	+00 28 24	1·1 p	0·1 s	17	7·59	−1·00	27	DA 553	55	−35	$z = 1·94$ (28), inverted spectrum
2216−03	22 16 16·3	−03 50 43			16·4	1·04	−0·30	5, 10	4C−03·79	59	−47	$z = 0·901$ (21), h.f. enhancement
2254+024	22 54 44·6	+02 27 12	0·7 p	—	18	0·46	−0·20	9	OYO 91·3	76	−49	$z = 2·09$ (9), inverted spectrum
2318+02	23 18 15·0	+02 39 54	1·7 p	0·7 n	19	0·38	1·05	15	4C+02·58	83	−53	u.v.x.
2320−021	23 20 30·5	−02 07 09	0·4 p	0·2 n	19·5	0·33	0·05			79	−57	u.v.x.
2332−017	23 32 46·3	−01 47 47	1·1 p	—	18·5	0·64	0·40			84	−58	u.v.x.
2335−027	23 35 23·3	−02 47 39	0·6 p	0·1 n	19	0·60	−0·15			84	−60	u.v.x., h.f. enhancement
2340−036	23 40 22·5	−03 40 20	0·2 p	0·5 n	17	0·28	0·7			85	−61	u.v.x.

* For references see footnote at end of Table 2.

III. Identification Tables

Tables 2 and 3 give details of the identifications or suggested identifications in the selected areas and the $\pm 4°$ zone respectively. For the sake of completeness sources brighter than 0·3 f.u. which are in the selected areas within the $\pm 4°$ zone are included in both tables. The subheadings in Table 2 are the Palomar Plate numbers and the coordinates of the centres of these plates are listed in Table 1.

Column 1 in Tables 2 and 3 gives the Parkes catalogue number and column 10 other catalogue numbers for the source. Sources designated in column 1 by six-digit numbers occurred in the earlier Parkes catalogues, which were based on finding surveys at 408 MHz; sources which are exclusive to the 2700 MHz survey are distinguished by seven-digit numbers, the final number indicating tenths of degrees in declination.

Columns 2 and 3 give the optical positions of the identifications as estimated from the Sky Survey print with the aid of the transparent overlays. These estimated positions are probably accurate to $0' \cdot 1$ arc. Columns 4 and 5 give the displacement of the measured radio source position from the estimated optical position in right ascension and declination. For well-known QSOs for which accurate optical positions have been determined the precise positions are given in columns 2 and 3 and no displacements shown. These sources were used as position calibrators.

Column 6 contains an estimate of the visual magnitude m_V of the identification made from Sky Survey prints, or, where available from the literature in the case of a known identification, a photoelectric V magnitude. The latter is given to one-tenth of a magnitude and the former to half a magnitude.

Column 7 gives the flux density at 2700 MHz; the flux density is given in parentheses where it is known or thought to be variable.

Column 8 gives an estimate of the spectral index of the source in the vicinity of 2700 MHz; however, for many of the QSOs in the present list the spectral index is a function of frequency. For those sources whose spectra deviate markedly from power laws the remarks column (13) contains brief descriptions of the form of the spectrum.

Column 9 gives reference to the original identification of a known QSO and to the accurate determination of its optical position.

Columns 11 and 12 give the galactic latitude and longitude of the source.

Redshifts, where known, together with references in parentheses, are given in column 13; "u.v.x." and "u.v.x.?" indicate definite or probable ultraviolet excess, as discussed in Section II; "inverted spectrum" indicates that the maximum flux density occurs in the vicinity of 2700 MHz, "h.f. enhancement" (high-frequency) indicates that the spectral index numerically decreases towards the high-frequency end of the spectrum, and "l.f. cutoff" (low-frequency) indicates the possibility of synchrotron self-absorption towards the low-frequency end of the spectrum.

IV. Finding Charts

Finding charts for all the new identifications or possible identifications are given in Figures 2–14 in order of increasing right ascension (except for PKS 1203+011, which is in Fig. 14). These were prepared from the blue Sky Survey prints and the object is indicated by the two bars. The scale of the finding charts is approximately 5 mm = 1′ arc, and north-east is at the top left-hand corner.

V. Retractions of Previously Suggested Identifications

A number of possible identifications of Parkes catalogue sources in the $\pm 4°$ zone suggested by Bolton and Ekers (1966*b*, 1967) can be retracted on the basis of the present work. These are PKS 0013−00, 0047−02, 0458−02, 0854−03, 2121−01, and 2154−18. More precise radio positions eliminate PKS 0047−02 and 0854−03 and absence of ultraviolet excess eliminates the remainder. Positional agreement in the case of PKS 0458−02 is very good; it may be an N-galaxy. The identification for PKS 0300−00 originally suggested as a galaxy by Bolton and Ekers (1967) has been changed to a nearby QSO, as has the identification for PKS 0505+03 (Clarke, Bolton, and Shimmins 1966).

VI. Additional Redshifts

Redshifts for six of the QSOs in Table 3 were obtained by J.G.B. with the image-tube spectrograph at the prime focus of the 120 in. telescope at the Lick Observatory in November 1968. The sources are listed below, together with the measured wavelengths of emission lines in their spectra, the rest wavelength of the line identification (in parentheses), and the redshift z.

PKS 0038−020 : 4154 (λ1909), 6096 (λ2798), $z = 1\cdot176$,

0118+03 : 4939 (λ2798), 6043 (λ3426), 6575 (λ3727), 6844 (λ3869), $z = 0\cdot765$,

0226−038 : 4743 (λ2798), $z = 0\cdot695$,

0336−01 : 5182 (λ2798), $z = 0\cdot852$,

0420−01 : 5355 (λ2798), 6564 (λ3426), $z = 0\cdot915$,

0421+019 : 4726 (λ2798), 5794 (λ3426), $z = 0\cdot689$.

The redshifts for two of the sources depend on the identification of only one strong emission line as MgII (λ2798). Alternative identifications with either Ly-α (λ1216) or CIV (λ1549) can almost certainly be excluded by the absence of other strong lines within the range of the spectra.

VII. Relationships between Various QSO Parameters

The present sample contains sufficient QSOs to warrant a brief examination of the relationships between the various radio and optical parameters.

(*a*) *Radio Spectra and Flux Densities*

For most of the sources in the $\pm 4°$ zone, measurements of flux density were made at 468, 635, 1410, 2700, and 5000 MHz. About half the sources have complex spectra which cannot be represented by a simple power law over a wide frequency range. Thus a spectral index appropriate to the region of the survey frequency,

Figs 2–14.—Finding charts for the QSOs. The scale is 5 mm ≈ 1′ arc and north-east is at the top left-hand corner of each chart.

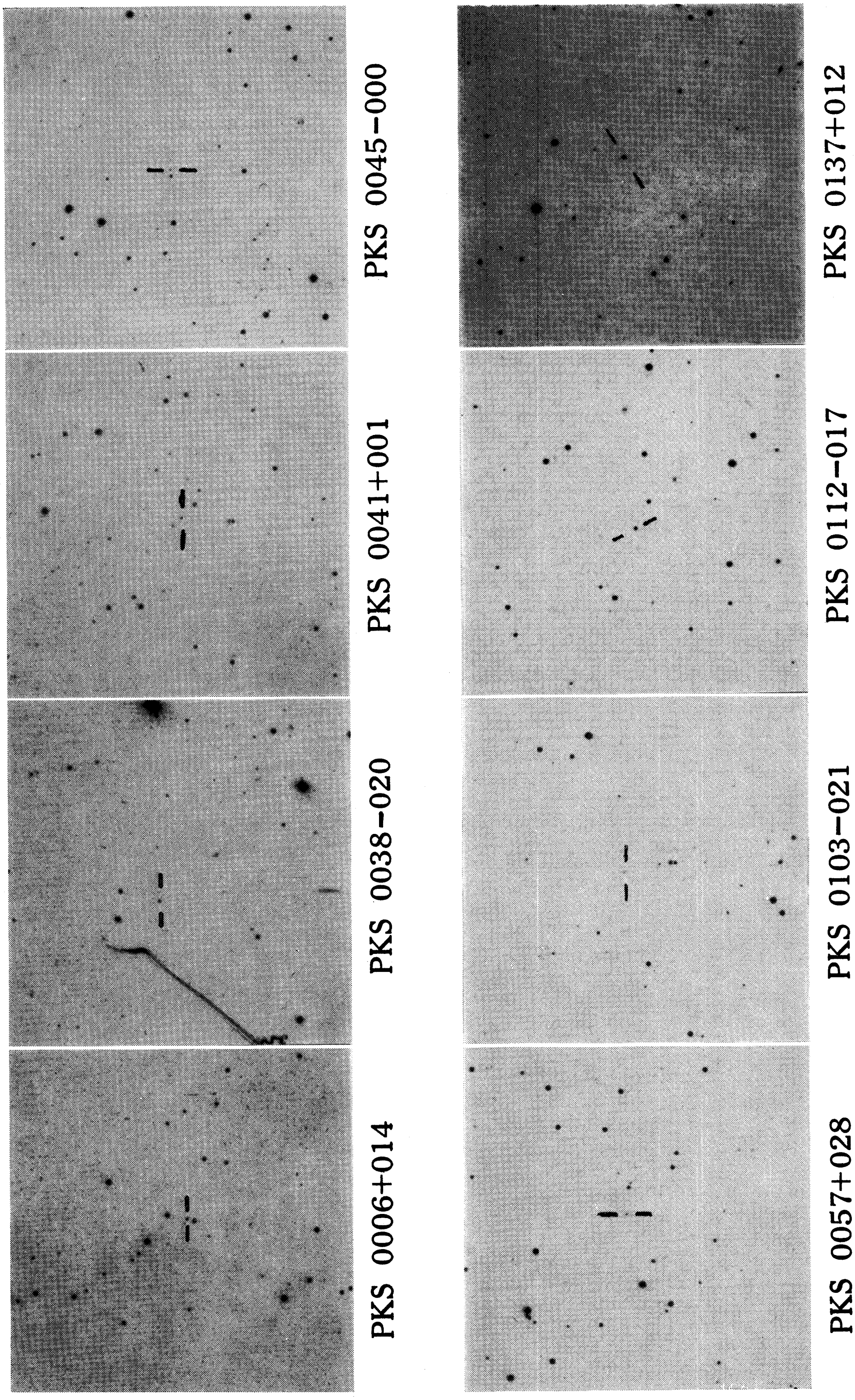
PKS 0045−000
PKS 0041+001
PKS 0038−020
PKS 0006+014
PKS 0137+012
PKS 0112−017
PKS 0103−021
PKS 0057+028

Fig. 2

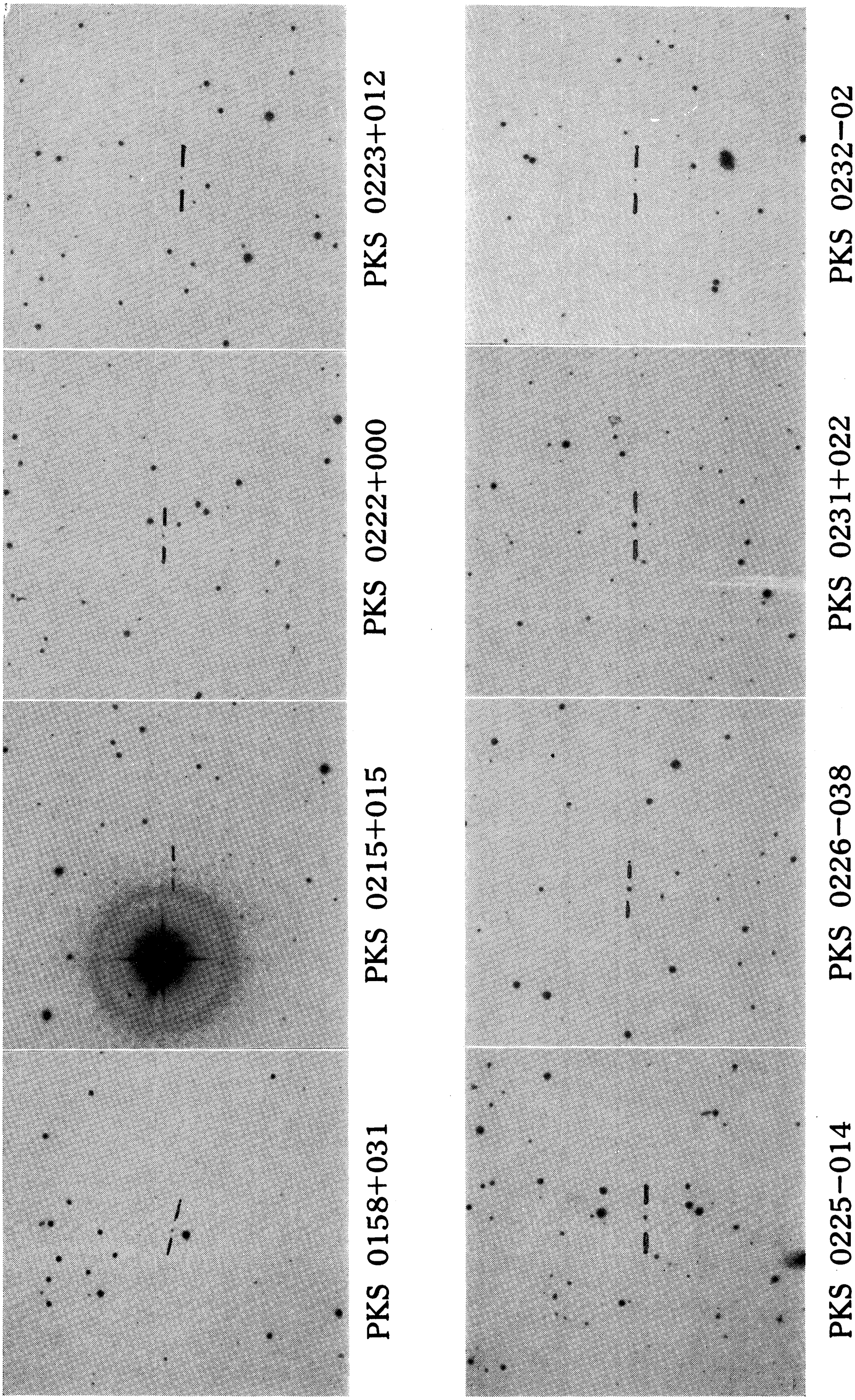
PKS 0158+031
PKS 0215+015
PKS 0222+000
PKS 0223+012
PKS 0225−014
PKS 0226−038
PKS 0231+022
PKS 0232−02

Fig. 3

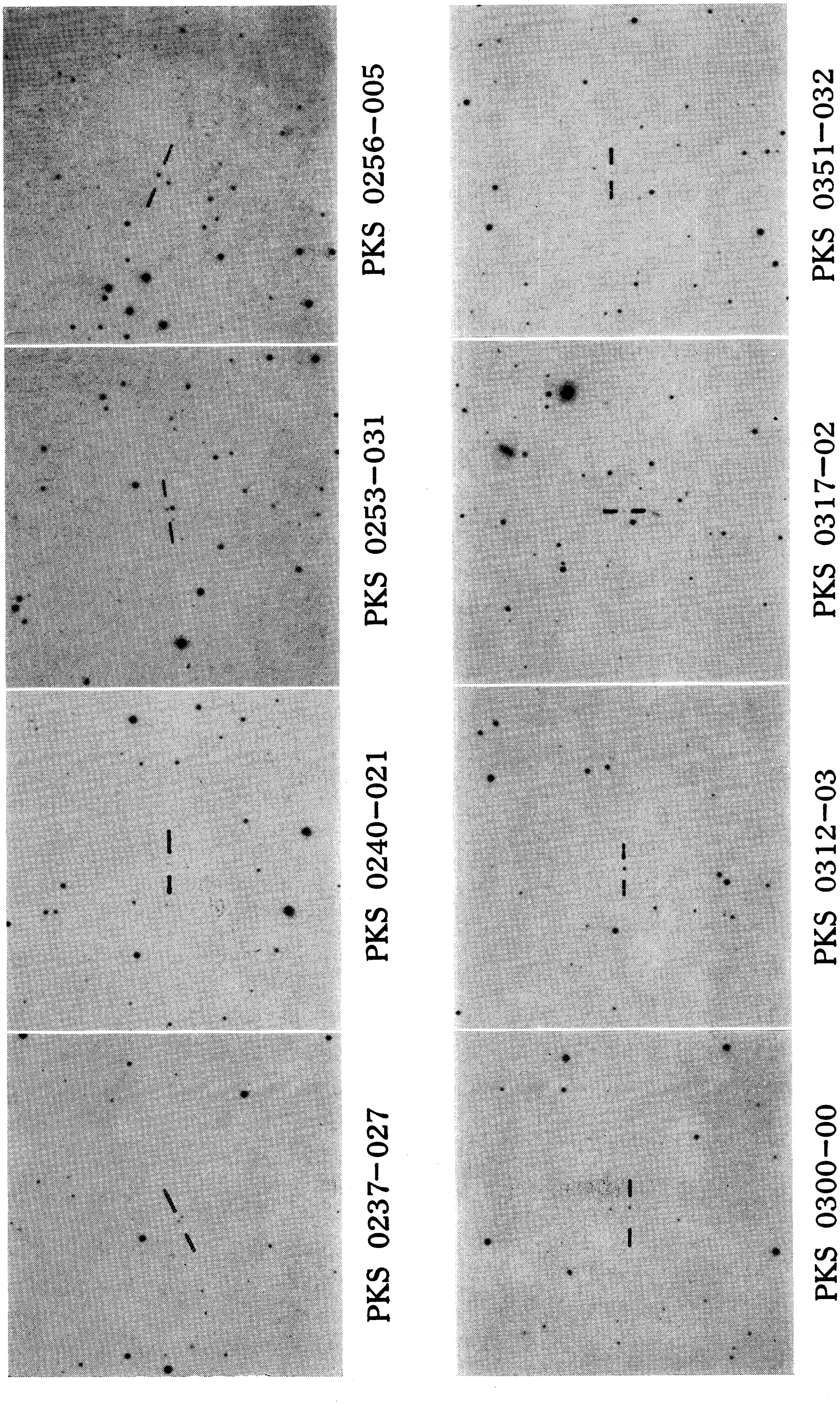
PKS 0256−005
PKS 0253−031
PKS 0240−021
PKS 0237−027
PKS 0351−032
PKS 0317−02
PKS 0312−03
PKS 0300−00

Fig. 4

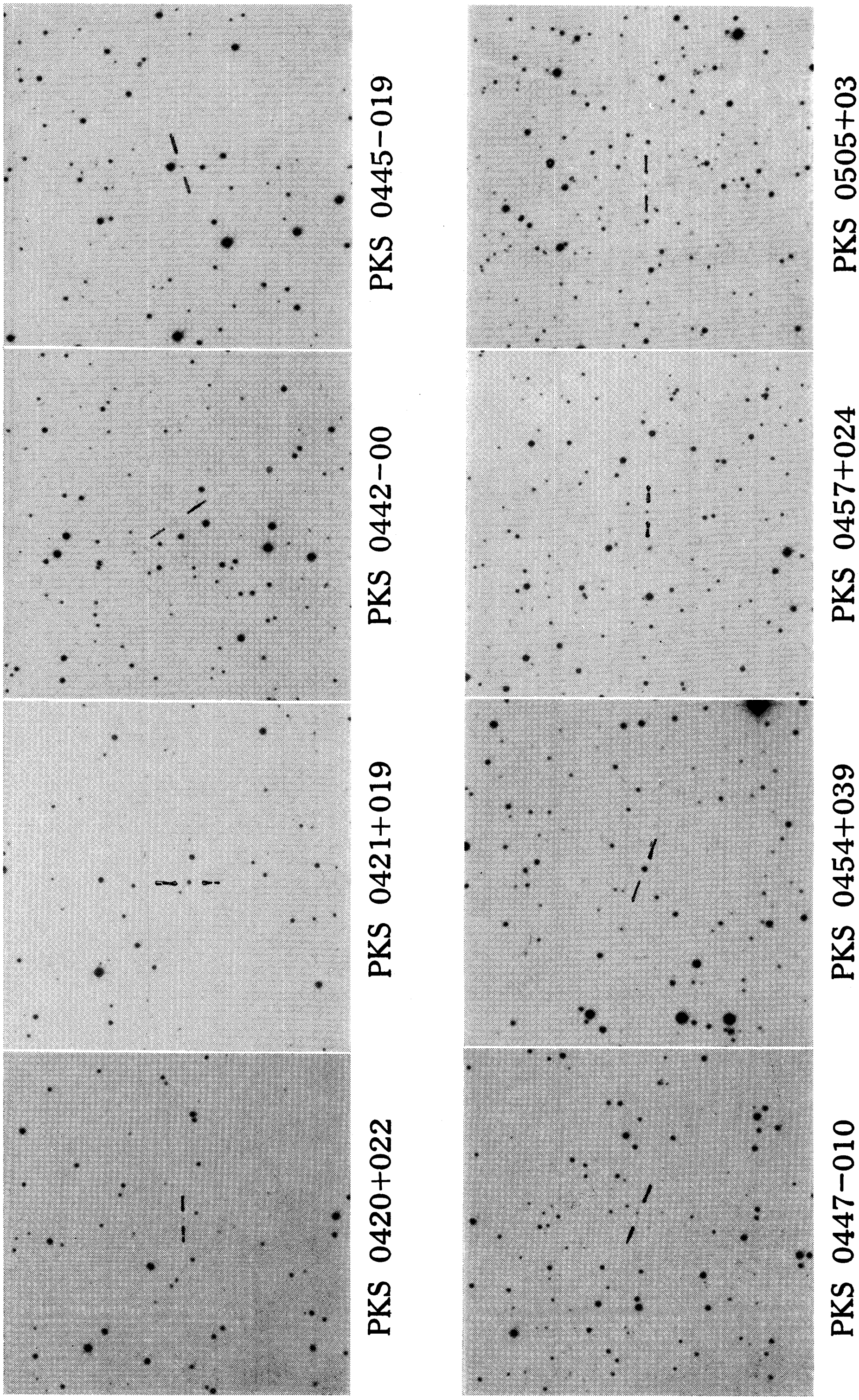
PKS 0445−019
PKS 0442−00
PKS 0421+019
PKS 0420+022
PKS 0505+03
PKS 0457+024
PKS 0454+039
PKS 0447−010

Fig. 5

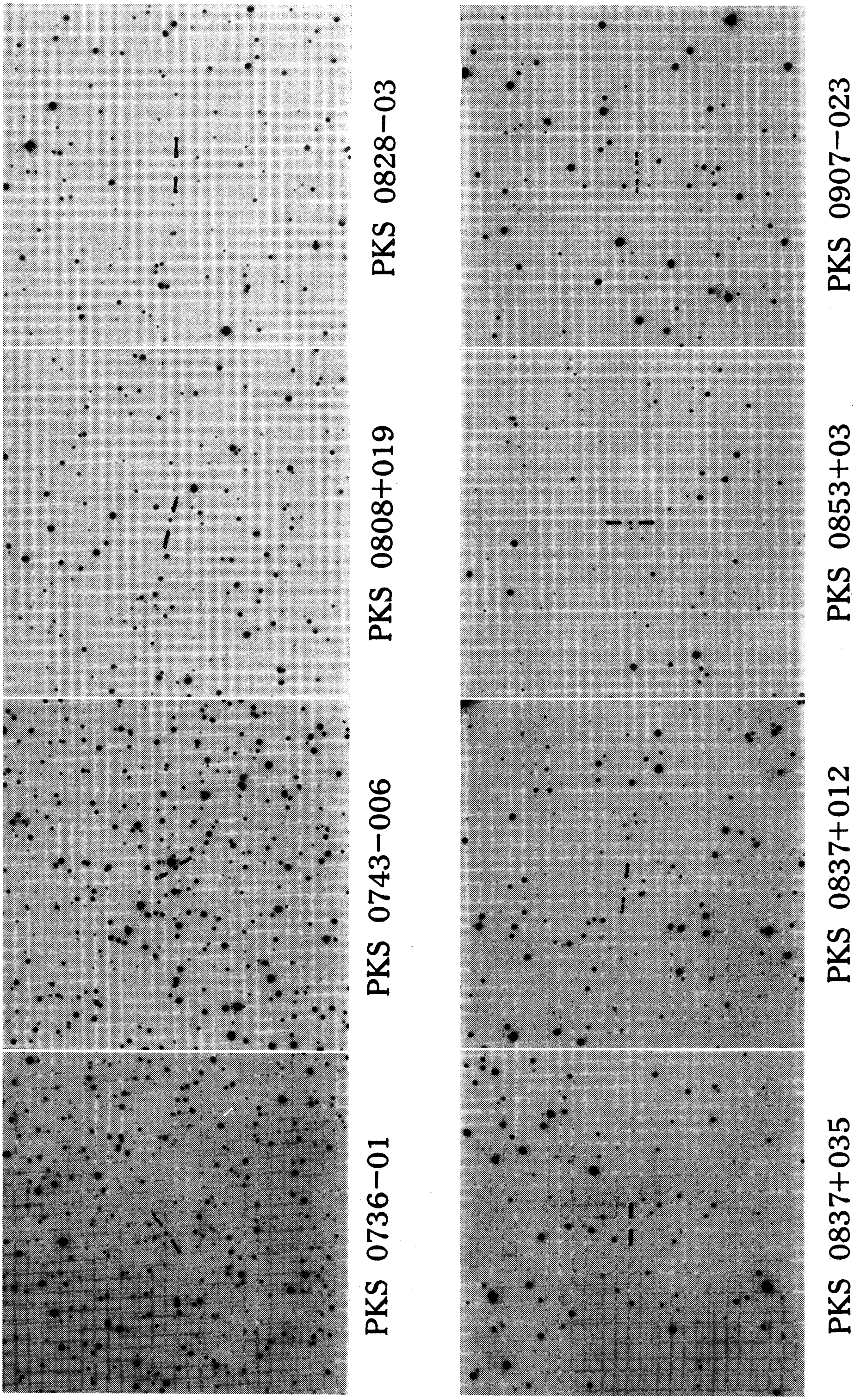
PKS 0828−03
PKS 0808+019
PKS 0743−006
PKS 0736−01
PKS 0907−023
PKS 0853+03
PKS 0837+012
PKS 0837+035

Fig. 6

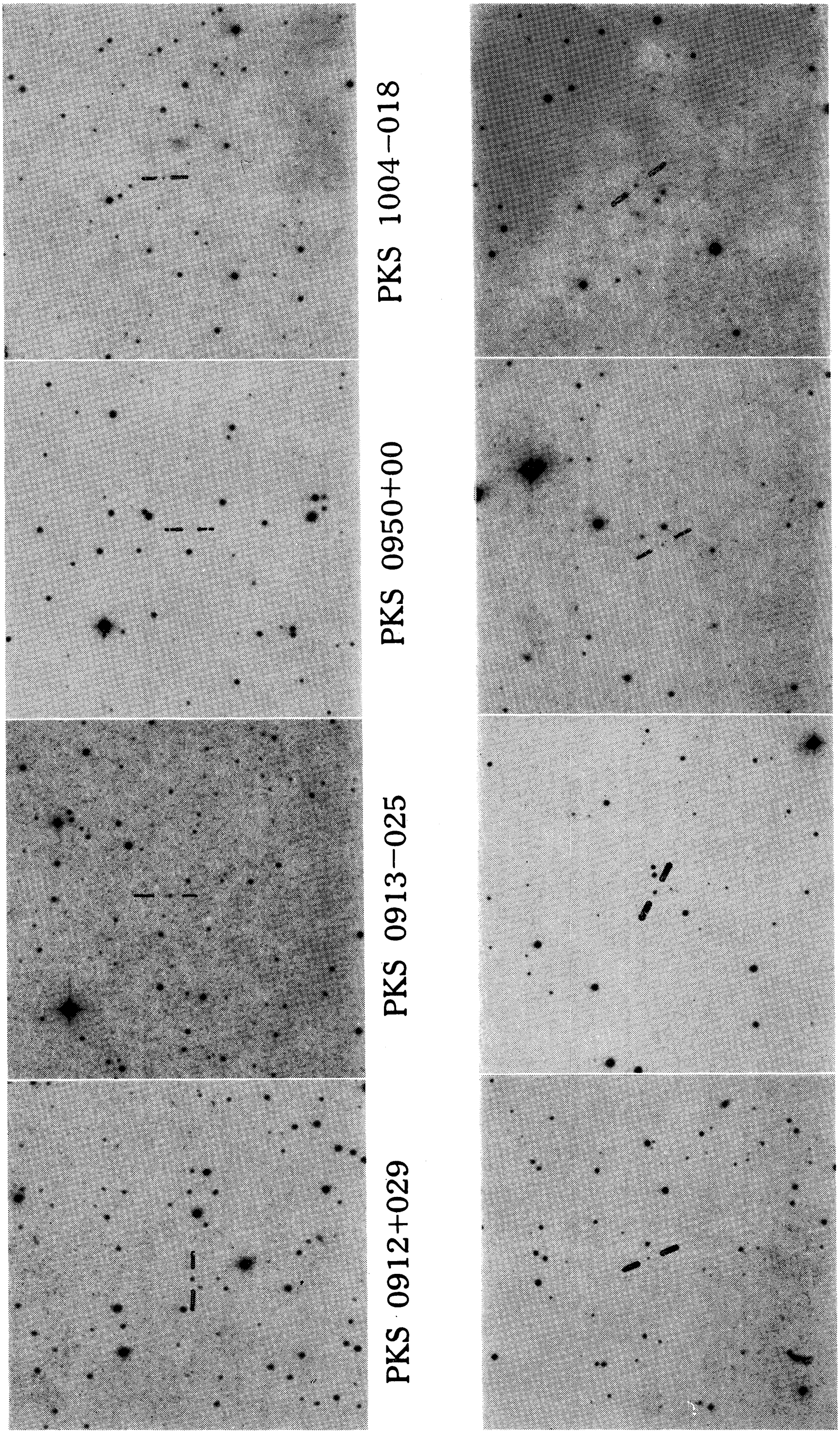
PKS 1004−018
PKS 0950+00
PKS 0913−025
PKS 0912+029
PKS 1052−004
PKS 1021+028
PKS 1012+022
PKS 1008+013

Fig. 7

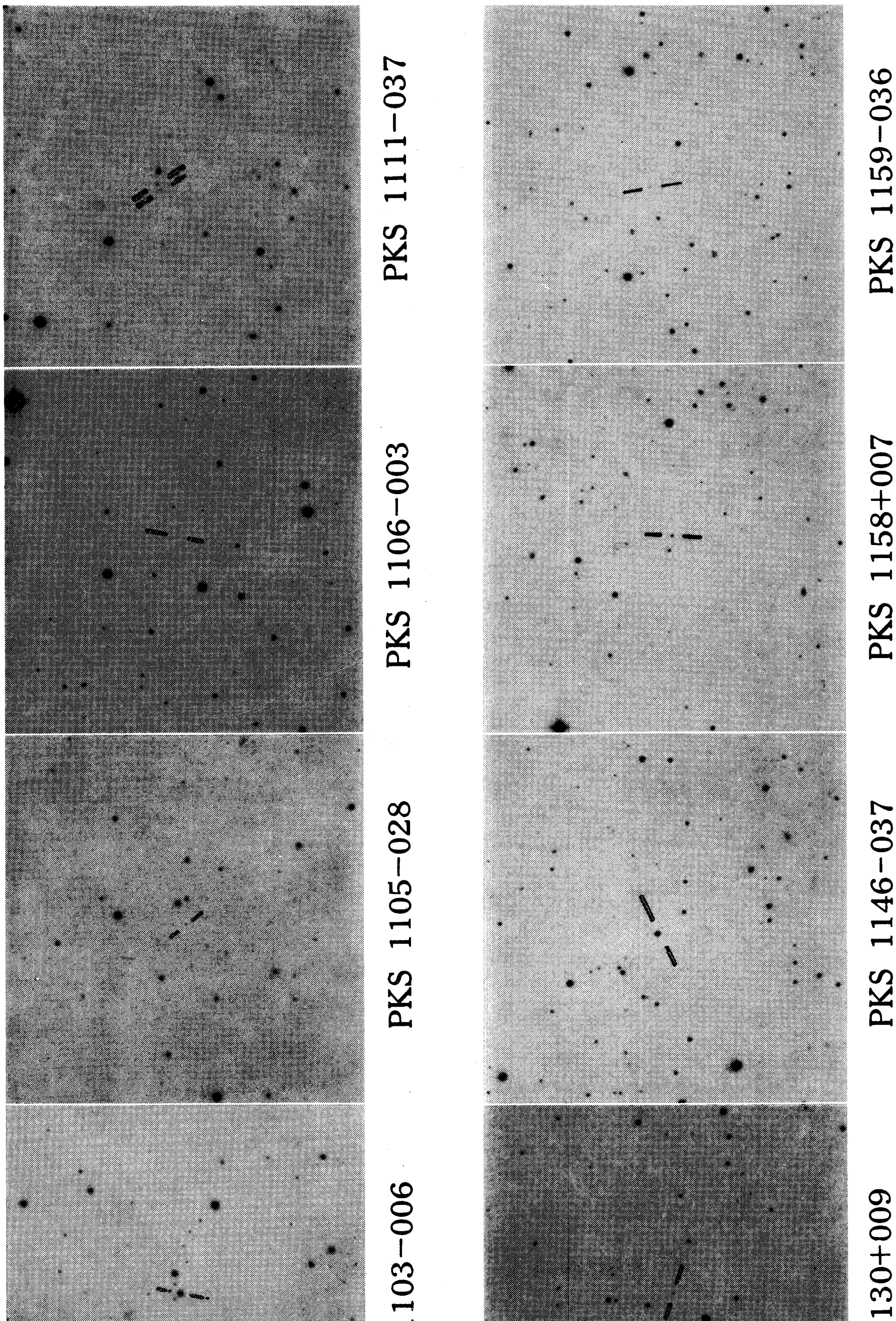
PKS 1111−037
PKS 1106−003
PKS 1105−028
PKS 1103−006
PKS 1159−036
PKS 1158+007
PKS 1146−037
PKS 1130+009

Fig. 8

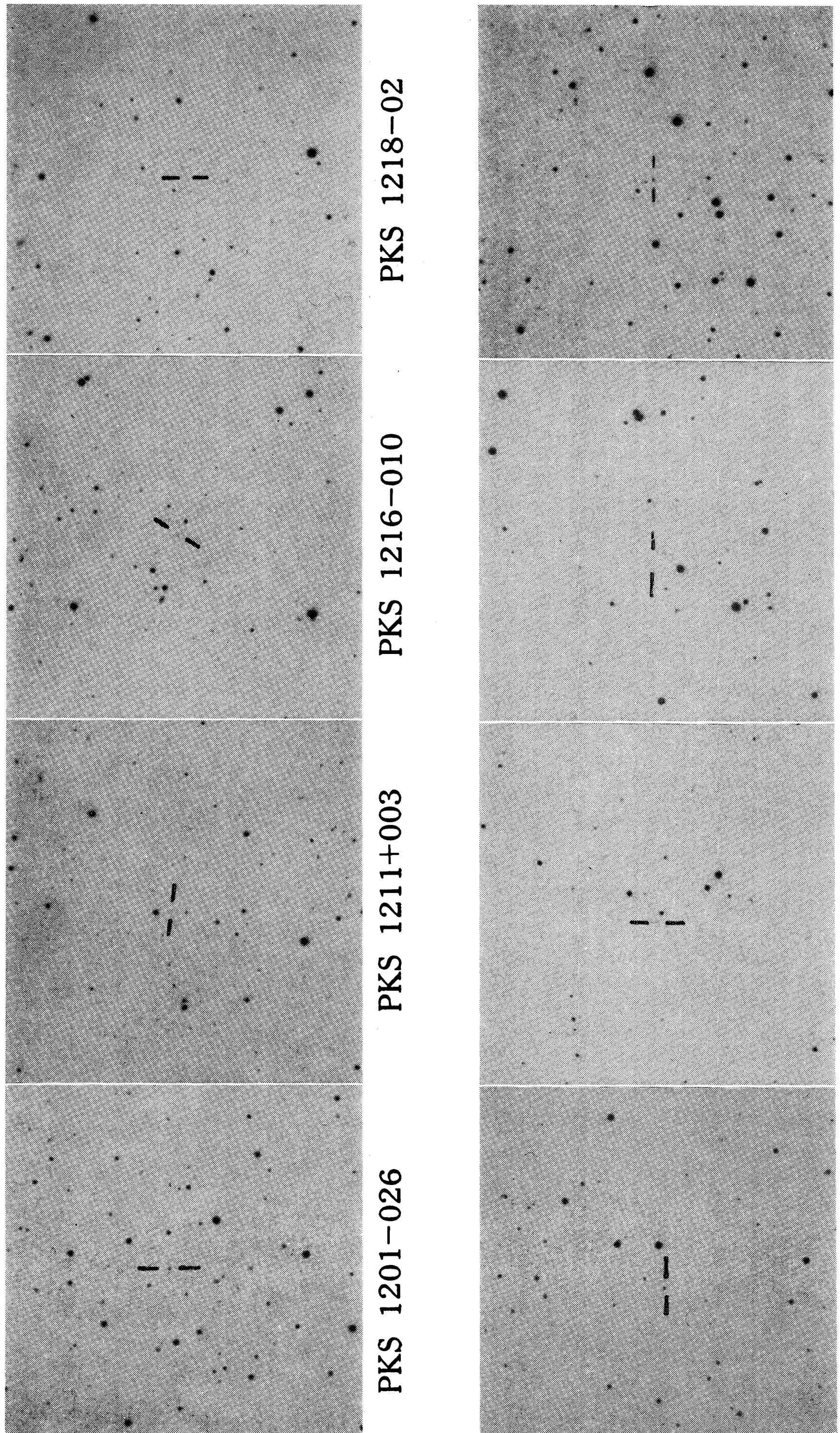
PKS 1201−026
PKS 1211+003
PKS 1216−010
PKS 1218−02
PKS 1222+037
PKS 1225−02
PKS 1302−035
PKS 1328−034

Fig. 9

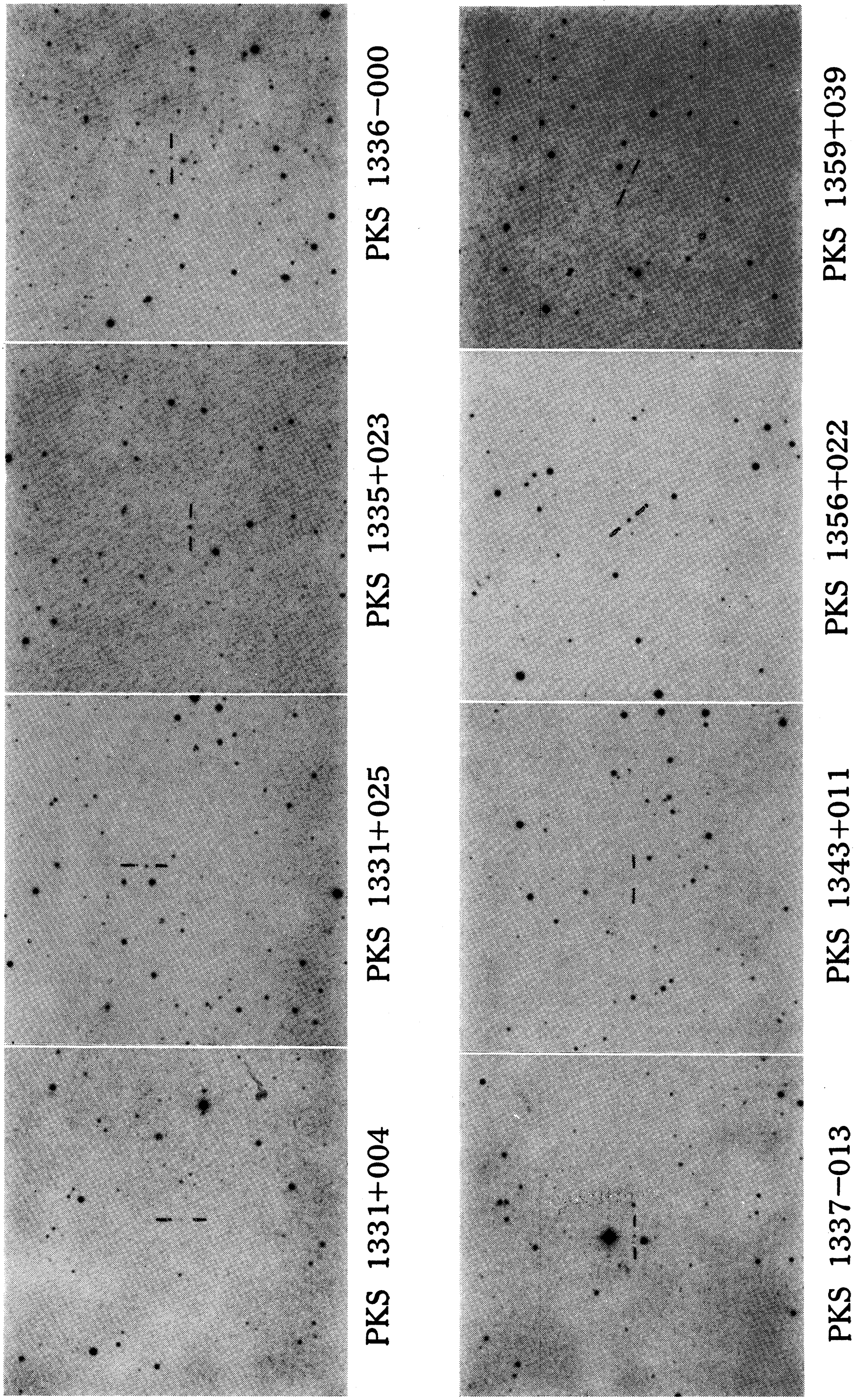
PKS 1331+004
PKS 1331+025
PKS 1335+023
PKS 1336−000
PKS 1337−013
PKS 1343+011
PKS 1356+022
PKS 1359+039

Fig. 10

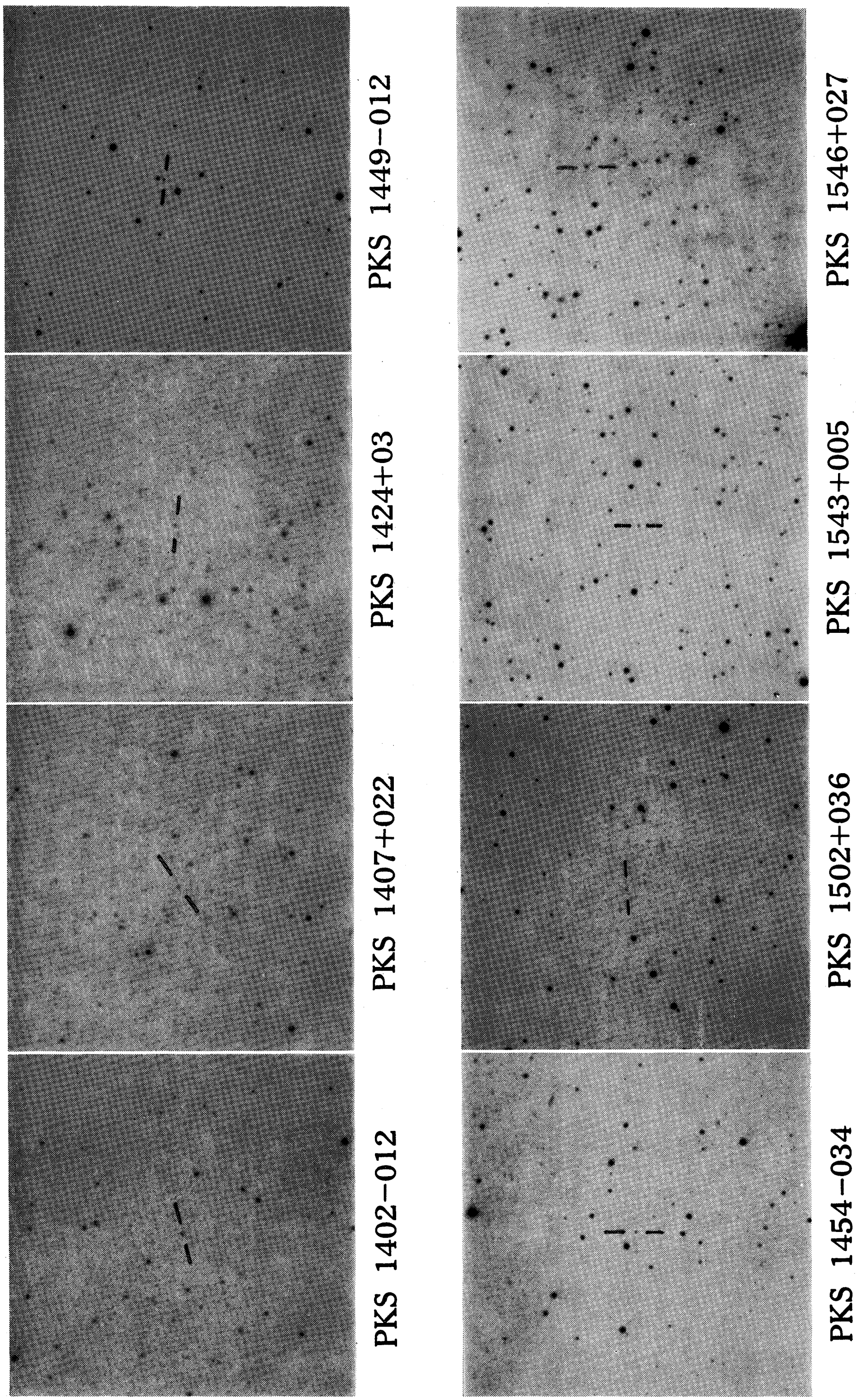
PKS 1449−012
PKS 1424+03
PKS 1407+022
PKS 1402−012
PKS 1546+027
PKS 1543+005
PKS 1502+036
PKS 1454−034

Fig. 11

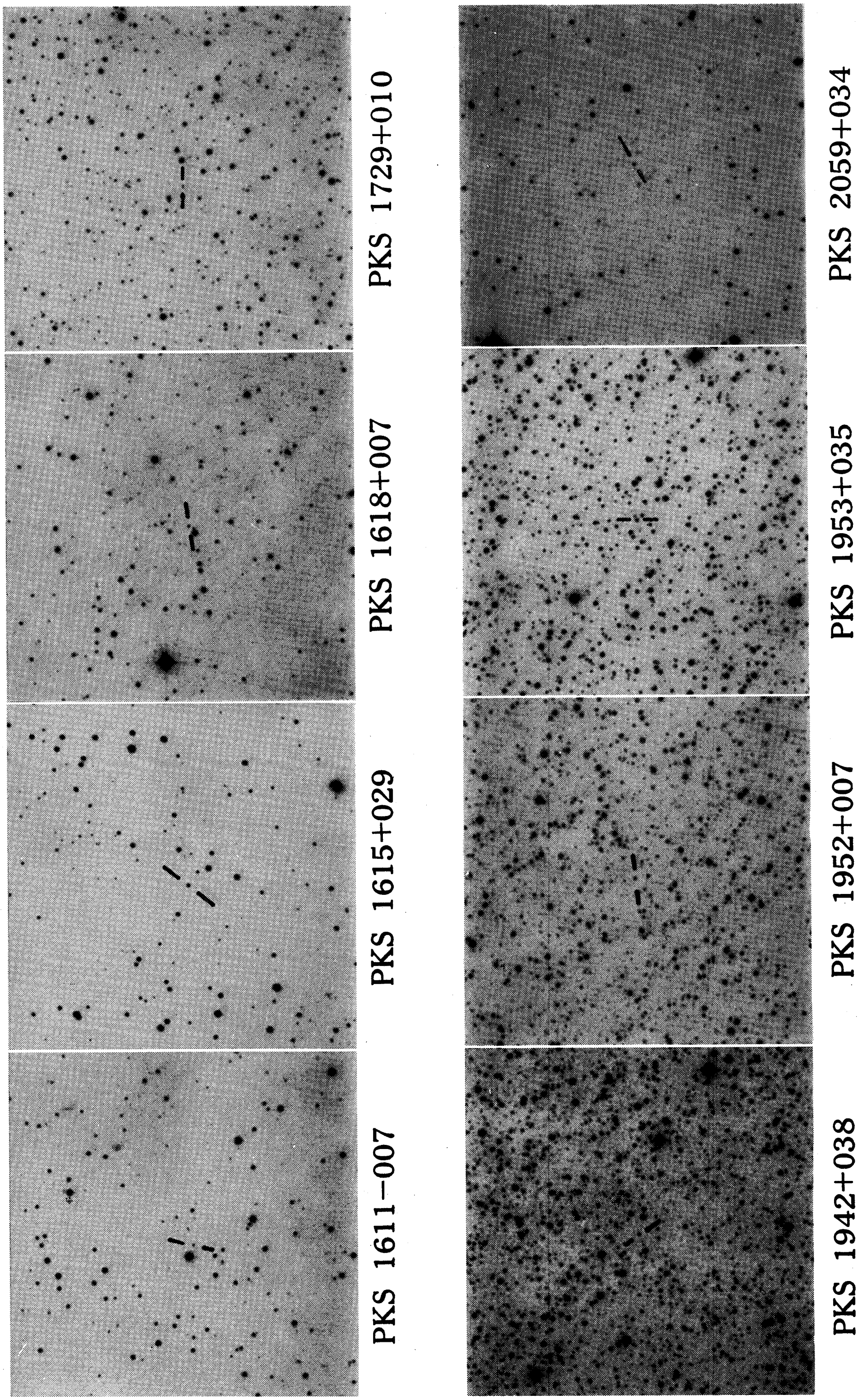
PKS 1611−007
PKS 1615+029
PKS 1618+007
PKS 1729+010
PKS 1942+038
PKS 1952+007
PKS 1953+035
PKS 2059+034

Fig. 12

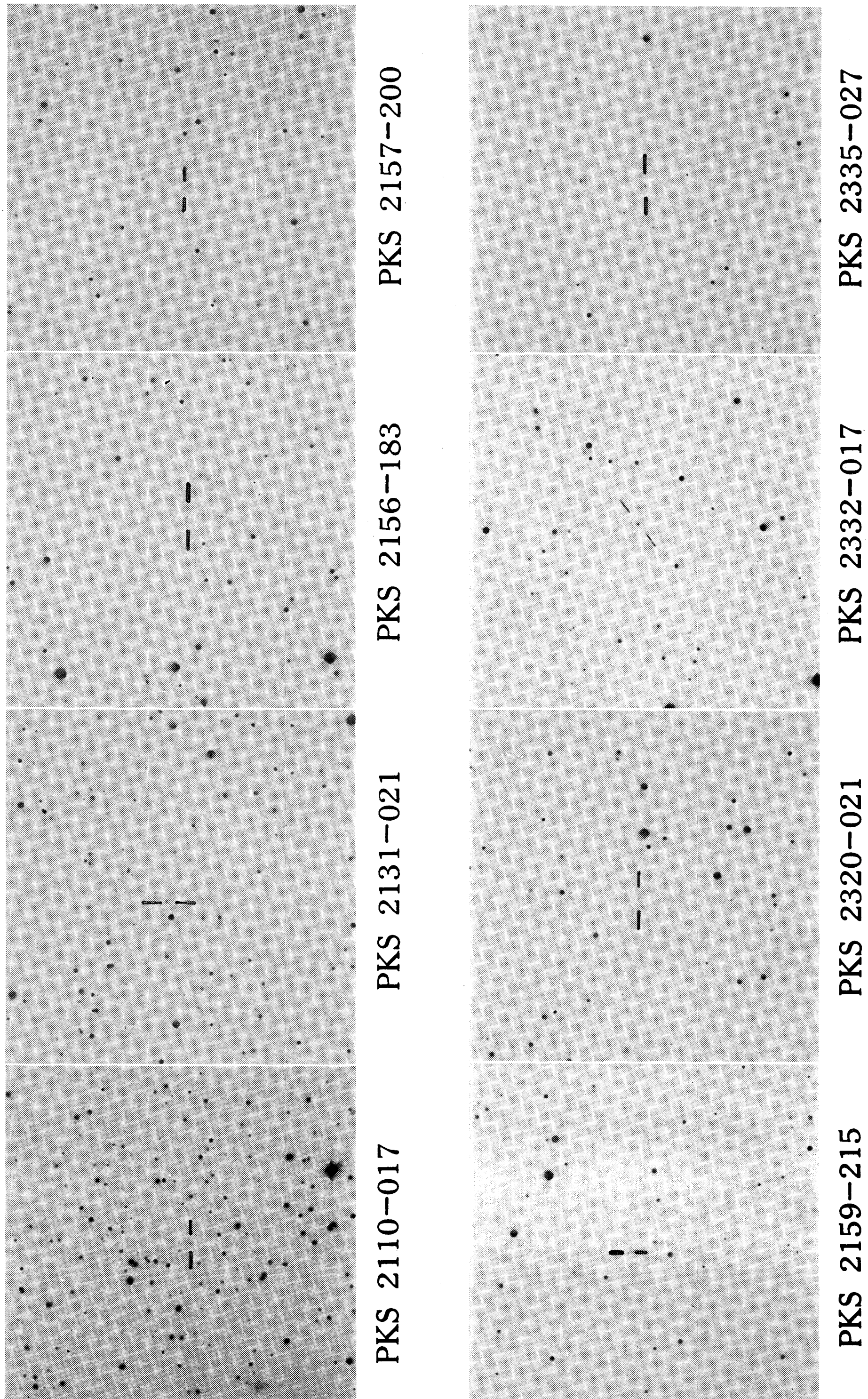
PKS 2157−200
PKS 2156−183
PKS 2131−021
PKS 2110−017
PKS 2335−027
PKS 2332−017
PKS 2320−021
PKS 2159−215

Fig. 13

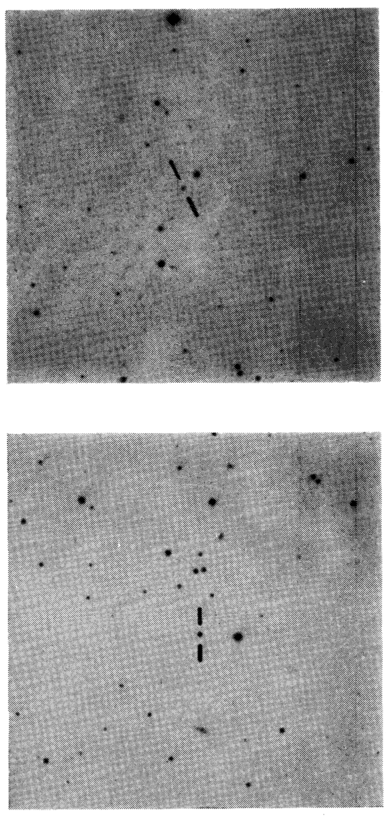

PKS 1203+011

PKS 2340−036

Fig. 14

2700 MHz, is given in the identification tables. A histogram of these spectral indices is shown in Figure 15. The distribution is remarkably broad when compared with either the distribution for QSO spectral indices found from low-frequency radio catalogues or the distribution of spectral indices for radio galaxies found from radio catalogues at any frequency. The median spectral index (defined by $S_\nu = \nu^{-\alpha}$)

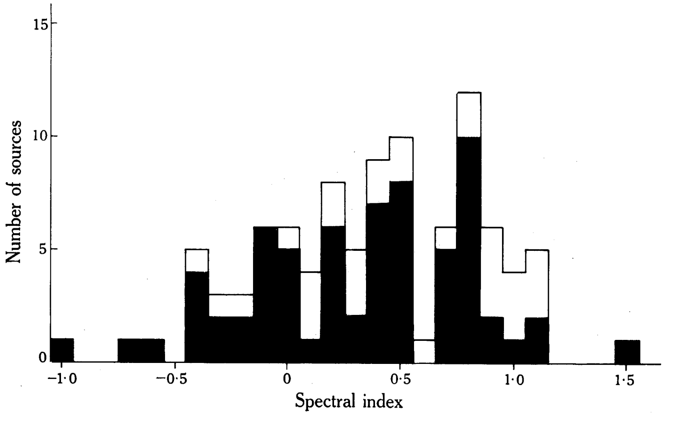

Fig. 15.—Distribution of the spectral indices at 2700 MHz of the QSOs and possible QSOs in the ±4° zone. QSOs with confirmed ultraviolet excess are shown in black.

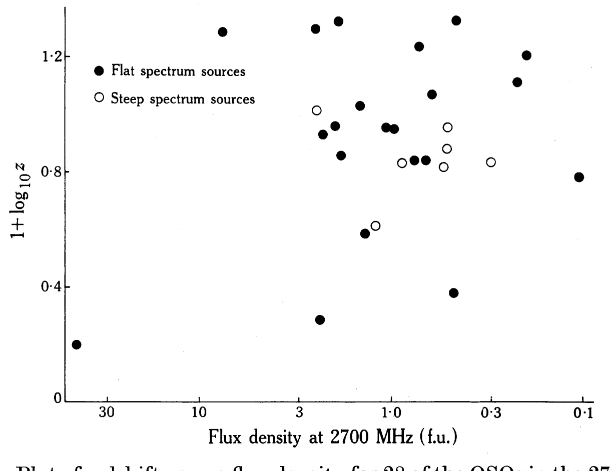

Fig. 16.—Plot of redshift versus flux density for 28 of the QSOs in the 2700 MHz survey. QSOs with spectral indices at 2700 MHz lower than 0·5 are shown as solid circles.

for radio galaxies is generally found to be $\sim 0 \cdot 85$ and the dispersion $0 \cdot 15$. The median spectral index for the sample in Figure 15 is $0 \cdot 4$; however, there is a considerable change in the median spectral index with flux density. The value for half the sample with $S_{2700} > 0 \cdot 55$ f.u. is $0 \cdot 2$, whereas the value for the half with $S < 0 \cdot 55$ is $0 \cdot 7$. (Excluding those objects which are not confirmed by a known u.v. excess, the values are $0 \cdot 2$ and $0 \cdot 5$.) This change in the median spectral index is not unexpected, since at the lower flux densities the sample should include a higher fraction of the steep spectrum QSOs which are abundant in the low-frequency catalogues, e.g. the QSOs in the 4C catalogue with $6 > S > 2 \cdot 5$ f.u. at 178 MHz for which Wills and Bolton (1969) found a median spectral index of 0·77 between 178 and 2700 MHz.

(*b*) *Redshift–Flux Density Relationship*

On the basis of rather limited data then available from the Parkes catalogue, Bolton (1966) suggested that there might be a relationship between the redshift and flux density for the flat spectrum (spectral index $\leqslant 0 \cdot 5$) QSOs. Redshifts have been measured for 28 of the sources only; however, their range in flux density covers

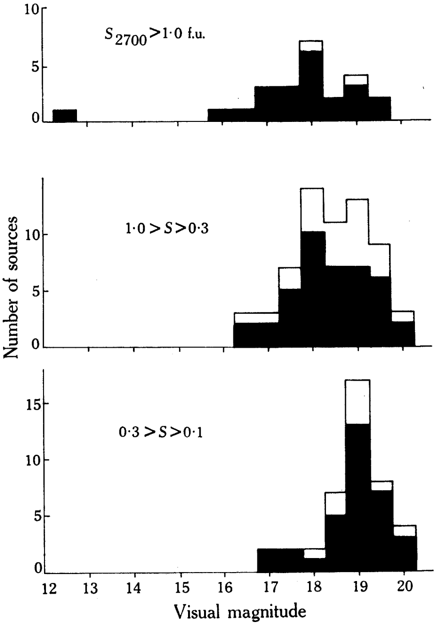

Fig. 17.—Histograms of the visual magnitudes m_V of the QSOs in the $\pm 4°$ zone and the selected areas for three ranges of flux density. Objects with confirmed ultraviolet excess are shown in black.

two orders of magnitude. In Figure 16 the redshifts are plotted against flux density at 2700 MHz. The addition of a number of high flux density QSOs with high redshifts and low flux density QSOs with low redshifts to the data available in 1966 has clearly destroyed any relationship between the two quantities.

(*c*) *Flux Density–Visual Magnitude Relationship*

The existence of intense radio sources which are optically faint QSOs and bright QSOs which are radio-quiet to the limit of existing radio telescopes made it clear that there is a large dispersion in the ratio of power emitted at radio and optical frequencies. Nevertheless a trend in the median visual magnitude with flux density might be expected, provided the observed range of flux densities is sufficiently large. Such a trend is just apparent in Figure 17, where histograms of the visual magnitudes of the QSOs in the present sample are shown for three ranges of flux density. The median visual magnitude changes from $m_V = 18$ to $m_V = 19$ for a change of a factor of 10 in the median flux density. The fact that this change is not greater suggests that at least for the two lower flux density groups there are significant tails to the distributions which extend beyond the plate limit of the Sky Survey. Wall (1970) has concluded from a study of the spectral characteristics of the unidentified sources in unobscured areas of the $\pm 4°$ zone that probably 25% of the unidentified sources with $S_{2700} > 0 \cdot 3$ f.u. are QSOs beyond the limit of the Sky Survey. Distribution of these objects within the appropriate flux ranges would tend to produce a more rapid variation in the median visual magnitude with flux density.

(*d*) *log N – log S Relationship*

A composite $\log N - \log S$ diagram for the QSOs in the $\pm 4°$ zone and the selected areas is shown in Figure 18. The data from the selected areas have been scaled up by a factor of 10, since the selected areas have one-tenth the area of the main survey.

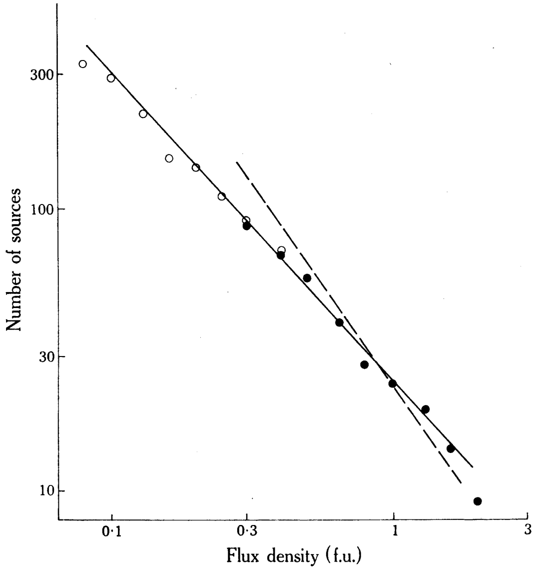

Fig. 18.—Diagram of $\log N - \log S$ for the QSOs in the $\pm 4°$ zone and the selected areas. Source counts from the $\pm 4°$ zone are shown as solid circles and those from the selected areas as open circles. The $\pm 4°$ zone has an area of $0 \cdot 75$ steradians.

The solid line drawn through the data points has a slope of $-1 \cdot 1$. This is very much lower than the slope found for either the Cambridge 178 MHz or Parkes 408 MHz survey and reflects the influence of the higher fraction of flat or inverted spectrum objects amongst the strong sources. Wall (1970) has suggested that 25% of the unidentified sources at a level of $0 \cdot 3$ f.u. are QSOs, and the dashed line has been drawn through a point at $S = 0 \cdot 3$ which allows for the inclusion of these objects. The slope of the dashed line is $-1 \cdot 45$, which is that derived for the number–flux density relation at 2700 MHz for all sources by Wall, Shimmins, and Merkelijn in the catalogue for the $\pm 4°$ zone which is in preparation. It is clear that the inclusion of QSOs beyond the plate limit cannot raise the initial $\log N - \log S$ slope to the value of $\sim -1 \cdot 8$ obtained from low-frequency surveys.

VIII. Acknowledgments

We would like to thank Miss Jeannette K. Merkelijn for assistance in examining the Sky Survey prints. J.G.B. wishes to thank Dr. H. Babcock for permission to use the 48 in. Schmidt telescope at Mount Palomar Observatory to obtain the two-colour plates and Dr. R. Kraft for permission to use the 120 in. telescope at the Lick Observatory to obtain spectra of some of the QSOs. J.V.W. acknowledges receipt of an A.N.U. Research Scholarship during this work.

Note added in proof

Two-colour (blue and u.v.) photography with the image tube camera at the Cassegrain focus of the Mount Stromlo 74 in. telescope by Dr. B. A. Peterson and the authors has confirmed ultraviolet excess for the following objects:

PKS 1146−037, 1449−012, 1602−00·2, and 1615+029.

The following objects have probable ultraviolet excess:

PKS 1454−034 and 1546+027.

The brighter object noted in the remarks column of Table 3 as 0′·5 n.f. 1454−034 and the suggested identification for 1729+010 have no ultraviolet excess.

IX. References

Bolton, J. G. (1966).—*Nature, Lond.* **211**, 917.

Bolton, J. G. (1968).—*Publs astr. Soc. Pacif.* **80**, 5.

Bolton, J. G., Clarke, Margaret E., Sandage, A. R., and Véron, P. (1965).—*Astrophys. J.* **142**, 1289.

Bolton, J. G., and Ekers, Jennifer A. (1966*a*).—*Aust. J. Phys.* **19**, 471.

Bolton, J. G., and Ekers, Jennifer A. (1966*b*).—*Aust. J. Phys.* **19**, 559.

Bolton, J. G., and Ekers, Jennifer A. (1966*c*).—*Aust. J. Phys.* **19**, 713.

Bolton, J. G., and Ekers, Jennifer A. (1967).—*Aust. J. Phys.* **20**, 109.

Bolton, J. G., and Kinman, T. D. (1966).—*Astrophys. J.* **145**, 951.

Bolton, J. G., Kinman, T. D., and Wall, J. V. (1968).—*Astrophys. J.* **154**, L105.

Bolton, J. G., Shimmins, A. J., Ekers, Jennifer A., Kinman, T. D., Lamla, E., and Wirtanen, C. A. (1966).—*Astrophys. J.* **144**, 1229.

Bolton, J. G., Shimmins, A. J., and Merkelijn, Jeannette K. (1968).—*Aust. J. Phys.* **21**, 81.

Bolton, J. G., and Wall, J. V. (1969).—*Astrophys. Lett.* **3**, 177.

Burbidge, E. Margaret (1966).—*Astrophys. J.* **143**, 612.

Burbidge, E. Margaret, and Kinman, T. D. (1966).—*Astrophys. J.* **145**, 654.

Clarke, Margaret E., Bolton, J. G., and Shimmins, A. J. (1966).—*Aust. J. Phys.* **19**, 375.

Hazard, C., Mackey, M. B., and Shimmins, A. J. (1963).—*Nature, Lond.* **197**, 1037.

Jefferys, W. H., III (1964).—*Astr. J.* **69**, 255.

Kinman, T. D., Bolton, J. G., Clarke, R. W., and Sandage, A. R. (1967).—*Astrophys. J.* **147**, 848.

Kinman, T. D., and Burbidge, E. Margaret (1967).—*Astrophys. J.* **148**, L59.

Lynds, C. R. (1967).—*Astrophys. J.* **147**, 837.

Lynds, C. R., Hill, S. J., Heere, Karen, and Stockton, A. N. (1966).—*Astrophys. J.* **144**, 1244.

Merkelijn, Jeannette K. (1969).—*Aust. J. Phys.* **22**, 237.

Merkelijn, Jeannette K., and Wall, J. V. (1970).—*Aust. J. Phys.* **23**, 575.

Sandage, A. R., Véron, P., and Wyndham, J. D. (1965).—*Astrophys. J.* **142**, 1307.

Schmidt, M. (1963).—*Nature, Lond.* **197**, 1040.

Searle, L., and Bolton, J. G. (1968).—*Astrophys. J.* **154**, L101.

Shimmins, A. J., Bolton, J. G., and Wall, J. V. (1968).—*Nature, Lond.* **217**, 818.

Shimmins, A. J., Searle, L., Andrew, B. H., and Brandie, G. W. (1968).—*Astrophys. Lett.* **1**, 167.

Smith, H. J., and Hoffleit, D. (1963).—*Nature, Lond.* **198**, 650.

Wall, J. V. (1970).—Ph.D. Thesis, Australian National University.

Wills, D., and Bolton, J. G. (1969).—*Aust. J. Phys.* **22**, 775.